Chemical Engineering Journal Advances 26 (2026) 101190

Contents lists available at ScienceDirect

Chemical Engineering Journal Advances

journal homepage: www.sciencedirect.com/journal/chemical-engineering-journal-advances

Structure-property relationships in dimeric metallosurfactants: counterion-driven modulation of rheology, wettability and antibacterial performance

Ana Ivančić [a], Krunoslav Bojanić [b], Mirna Perkušić [c], Ivana Tartaro Bujak [b], Katarina Marušić [b], Nives Novosel Vlašić [d], Tea Mišić Radić [d], Darija Domazet Jurašin [a,*]

[a] Division of Physical Chemistry, Ruđer Bošković Institute, HR-10000 Zagreb, Croatia
[b] Division of Materials Chemistry, Ruđer Bošković Institute, HR-10000 Zagreb, Croatia
[c] Department of Pharmaceutical Technology, Faculty of Pharmacy and Biochemistry, University of Zagreb, HR-10000 Zagreb, Croatia
[d] Division for Marine and Environmental Research, Ruđer Bošković Institute, HR-10000 Zagreb, Croatia

ARTICLE INFO

Keywords:
Metallosurfactants
Dimeric surfactants
Wettability
Wormlike micelles
Viscoelasticity
Antibacterial
Antibiofilm

ABSTRACT

The development of next-generation surface coatings benefits from surfactant systems whose interfacial and bulk properties can be tuned to achieve targeted functionalities. In this work, we examine the influence of tetrabromometallate counterions, $[MBr_4]^{2-}$ (M = Co, Ni, Cu, Zn), on the rheological, wetting, and antibacterial properties of dimeric metallosurfactants derived from bis(*N*,*N*-dimethyl-*N*-dodecyl)ethylene-1,2-diammonium dibromide (12-2-12). Dissociation of the complex counterions increases ionic strength and promotes micellar transitions from spherical to cylindrical to wormlike aggregates. This results in a pronounced increase in viscosity and viscoelasticity in the low millimolar concentration range, without added salts or co-surfactants.

Similarly, at the stainless steel interface, electrostatic screening reduces repulsion between quaternary ammonium headgroups, enabling tighter interfacial packing and improved wetting compared with the metal-free precursor.

Antibacterial assays demonstrate potent activity in the low micromolar range against both Gram-positive and Gram-negative bacteria. Antibacterial performance is primarily governed by the amphiphilic dication $(12\text{-}2\text{-}12)^{2+}$, as evidenced by comparable minimum inhibitory (MIC) and minimum bactericidal (MBC) concentrations across the metallosurfactants and parent surfactant. For all tested species, minimum biofilm eradication concentrations (MBEC) exceed biofilm prevention concentrations (BPC), highlighting the increased resilience of established biofilms while confirming antibiofilm efficacy at micromolar levels.

This combination of viscoelasticity, surface wettability, and antibacterial performance is relevant to coating applications through its impact on film retention, thickness control, and bioprotective functionality. The limited influence of the metal ion on these properties allows metal selection to introduce additional functionalities without compromising the fundamental performance of the surfactant.

1. Introduction

Surfactants are amphiphilic compounds that lower surface and interfacial tension due to their dual structure, containing both hydrophilic (lipophobic) and hydrophobic (lipophilic) moieties. They can self-assemble into a variety of nano- and micro-aggregates such as micelles, vesicles, and liquid crystalline phases, depending on their molecular structure and solution conditions [1]. These unique physicochemical properties make them indispensable in everyday applications as well as in numerous industrial and technological processes, most notably as cleaning agents [2]. Beyond their use as detergents, surfactants are used as emulsifiers, dispersants, foaming and wetting agents, corrosion inhibitors, disinfectants, antistatic agents, and viscosity modifiers [2–5].

Since the 1990s, dimeric (gemini) surfactants have proven highly efficient across various applications, due to their markedly improved physicochemical properties in both solution and the solid state,

* Corresponding author at: Division of Physical Chemistry, Ruđer Bošković Institute, Bijenička cesta 54, 10 000 Zagreb, Croatia.
E-mail addresses: aivancic@irb.hr (A. Ivančić), kbojanic@irb.hr (K. Bojanić), mirna.perkusic@pharma.unizg.hr (M. Perkušić), itartaro@irb.hr (I.T. Bujak), kmarusic@irb.hr (K. Marušić), nives.novosel@irb.hr (N.N. Vlašić), tmisic@irb.hr (T.M. Radić), djurasin@irb.hr (D.D. Jurašin).

https://doi.org/10.1016/j.ceja.2026.101190

Available online 10 April 2026
2666-8211/© 2026 The Author(s). Published by Elsevier B.V. This is an open access article under the CC BY license (http://creativecommons.org/licenses/by/4.0/).

compared to conventional single-chain surfactants [6–9]. Bis-quaternary ammonium halides represent the largest class of dimeric surfactants and are particularly effective antimicrobials, with multiple studies demonstrating their high potency against mature biofilms [4,7,8]. Moreover, due to their molecular architecture, dimeric surfactants exhibit self-assembly behaviour distinct from that of their monomeric analogues. Those with short and rigid spacers are especially notable for their unique aggregation behaviour [9–12]. Even a small increase in concentration can induce a change in micellar shape from spherical to elongated, wormlike micelles (WLMs), significantly influencing the rheological properties of their solutions. Due to their advantages, viscoelastic solutions of surfactant WLMs are widely used today as rheological modifiers in consumer products, including detergents, paints and coatings, pharmaceutical formulations, and lubricants, as well as emulsifiers [13,14].

More recently, metallosurfactants, amphiphilic compounds incorporating metal-containing counterions or coordination centres, have been explored as multifunctional analogues of conventional surfactants [15]. By combining the amphiphilic nature of conventional surfactants with the distinctive properties of metal complexes, they retain intrinsic adsorption and self-assembly abilities while exhibiting variable oxidation states, tunable colour, magnetism, and pH sensitivity. Metallosurfactants with transition metals, in particular, have been explored for their antibacterial [16–18], antifouling [19], anticorrosion [19,20], and magnetic properties [21,22].

Based on these considerations, a series of dimeric metallosurfactants, (12-2-12)[MBr$_4$] where 12-2-12 denotes bis(*N,N*-dimethyl-*N*-dodecyl) ethylene-1,2-diammonium cation and M denotes Co, Ni, Cu, or Zn, were characterized to establish structure-property relationships through (i) rheological behaviour (flow curves, zero-shear viscosity, viscoelasticity); (ii) wettability evaluation via contact angle measurements on stainless steel as a representative metallic surface; and (iii) assessment of antibacterial and antibiofilm activity via minimum inhibitory concentration (MIC), minimum bactericidal concentration (MBC), biofilm prevention concentration (BPC), minimum biofilm eradication concentration (MBEC), and time-kill assays against representative Gram-positive and Gram-negative bacteria. These properties are relevant to potential surface coating applications, where enhanced viscosity can help control film retention and thickness, improved wettability promotes substrate coverage, and antibacterial activity provides bioprotective functionality [23,24]. Our previous work demonstrated that these metallosurfactant systems exhibit lower critical micelle concentrations (cmc) compared to the parent surfactant and form low-dimensional magnetic systems in the solid state [21].

This work provides a systematic evaluation of the antibacterial and antibiofilm activity profiles, time-kill behaviour, and rheological properties of metallosurfactant systems. Incorporation of tetrabromometallate counterions enhances viscosity and viscoelasticity, extending these properties into the low millimolar concentration range. Furthermore, all metallosurfactants yield lower contact angles than the metal-free precursor, consistent with improved wetting efficiency and tighter packing at the solid-liquid interface. Notably, the tetrabromometallate counterion acts as an intrinsic electrolyte, enabling pronounced micellar growth and viscoelastic response without added salts and co-surfactants. In parallel, these compounds also exhibit potent antibacterial performance in the micromolar concentration range against both Gram-positive and Gram-negative species. Taken together, the combination of favourable rheological, interfacial, and biological properties, along with straightforward synthesis and high yields, makes these systems well suited for the subsequent development of coating formulations.

2. Experimental section

2.1. Materials

N,N,N′,N′-Tetramethylethylenediamine (≥ 99,5%, Sigma-Aldrich) and 1-Bromododecane (97%, Sigma-Aldrich) were used for synthesis of dimeric precursor, 12-2-12. Cobalt (II) bromide (≥ 97%, Thermo Scientific), nickel (II) bromide (≥ 98%, Sigma-Aldrich), copper (II) bromide (≥ 99%, Thermo Scientific) and zinc (II) bromide (≥ 98%, Thermo Scientific) were used for synthesis of dimeric metallosurfactants, (12-2-12)[MBr$_4$]. All the chemicals for synthesis were used without further purification. Absolute ethanol (Honeywell Riedel-de Haën), methanol (Kemika, Croatia), and acetonitrile (Kemika, Croatia) were used as solvents for the synthesis and purification of the products.

2.2. *Synthesis of dimeric metallosurfactants (12-2-12)[MBr$_4$]*

All dimeric metallosurfactants (12-2-12)[MBr$_4$] were synthesized via a two-step process. Initially, dimeric surfactant 12-2-12 was prepared in refluxing acetonitrile as described previously [25]. Corresponding metallosurfactants were prepared in high yield from a reaction between respective metal bromide ($CoBr_2$, $NiBr_2$, $CuBr_2$ and $ZnBr_2$) and 12-2-12 in 1:1 molar ratio as described previously [21]. Before further analyses, all synthesized compounds were recrystallized from methanol or acetonitrile. For compound characterization (CHN, FTIR) see the Supporting information.

2.3. Methods

Preparation of solutions. All the required solutions were prepared in MilliQ water using volumetric flasks. All the solutions were thermostated at 25°C before measurements.

Contact angle measurements. Contact angle measurements between 2.5 × 2.5 cm^2 stainless steel plates (SS AISI 304) and surfactant solutions were conducted using the sessile drop method with a DataPhysics Contact Angle System OCA25 goniometer equipped with an electronic multiple direct dosing system DDE/3 and controlled by the OCA25 Device Control software (DataPhysics Instruments, Germany).

Prior to measurements, the protective foil was removed and stainless steel plates were ultrasonicated in ethanol for 20 min and subsequently rinsed. No polishing, etching, or plasma treatment was applied to preserve a representative surface state. Plates were then dried under ambient conditions.

B. Braun Inkjet®-F 1 mL disposable syringes were used to dispense 10 μL aliquots of surfactant solution onto the stainless steel surface at the dispensing rate of 1 μL s^{-1}. For each surfactant solution concentration, contact angle measurement was performed in ten independent replicates, and values were recorded after allowing each drop to stabilize for 1 min, with mean values calculated. The measured contact angle values were compared within each concentration across all systems. Statistical analysis was performed using one-way analysis of variance (ANOVA) followed by Tukey's honestly significant difference (HSD) post hoc test. Each sample was measured in ten independent replicates ($n = 10$), and differences were considered statistically significant at $p < 0.05$.

Rheology measurements. Rheological measurements were performed using a Modular Compact Rheometer MCR 102 (Anton Paar GmbH, Graz, Austria) with integrated Peltier temperature control system (accuracy 0.01°C). Rotational rheological tests were conducted with a cone plate geometry (CP50; diameter 50 mm, cone angle 1°) while oscillatory rheological measurements were carried out using a parallel plate geometry (PP50; diameter 50 mm). Data analysis was performed using RheoCompass™ Light software, Version 1.23.403 (Anton Paar GmbH, Graz, Austria). Detailed description of flow curve determination, amplitude sweep test and frequency sweep test is given in Supporting information.

AFM measurements. AFM (atomic force microscopy) imaging of wormlike micelles was performed using a Multimode scanning probe microscope equipped with a NanoScope IIIa controller (Bruker, Billerica, MA, USA) and a vertical engagement (JV) 125 μm scanner. A detailed description of sample preparation and measurement conditions is provided in the Supporting information.

Antibacterial and antibiofilm activity assays. Antibacterial activity of the dimeric metallosurfactants was evaluated using the broth microdilution method to determine minimal inhibitory concentration (MIC) and minimal bactericidal concentration (MBC) in cation-adjusted Mueller-Hinton broth (CAMHB) according to EUCAST guidelines [26] with minor modifications. The bacterial panel included Bacillus subtilis ATCC 6633, Escherichia coli NCTC 12241, Staphylococcus aureus DSM 1104, and Pseudomonas aeruginosa DSM 22644. MIC was determined as the lowest concentration completely inhibiting bacterial growth, assessed both visually and spectrophotometrically at 600 nm (OD_{600}). MBC was determined as the lowest concentration killing 99.9% of bacteria [27,28].

Prevention of biofilm formation was evaluated according to [27,29] with minor modifications. Biofilm prevention concentration (BPC) was determined as the lowest concentration preventing biofilm formation (OD_{590} < ODc, where ODc = mean OD of negative control + three standard deviations). Biofilm eradication capacity was assessed by treating pre-formed 24 h biofilms with samples, and minimal biofilm

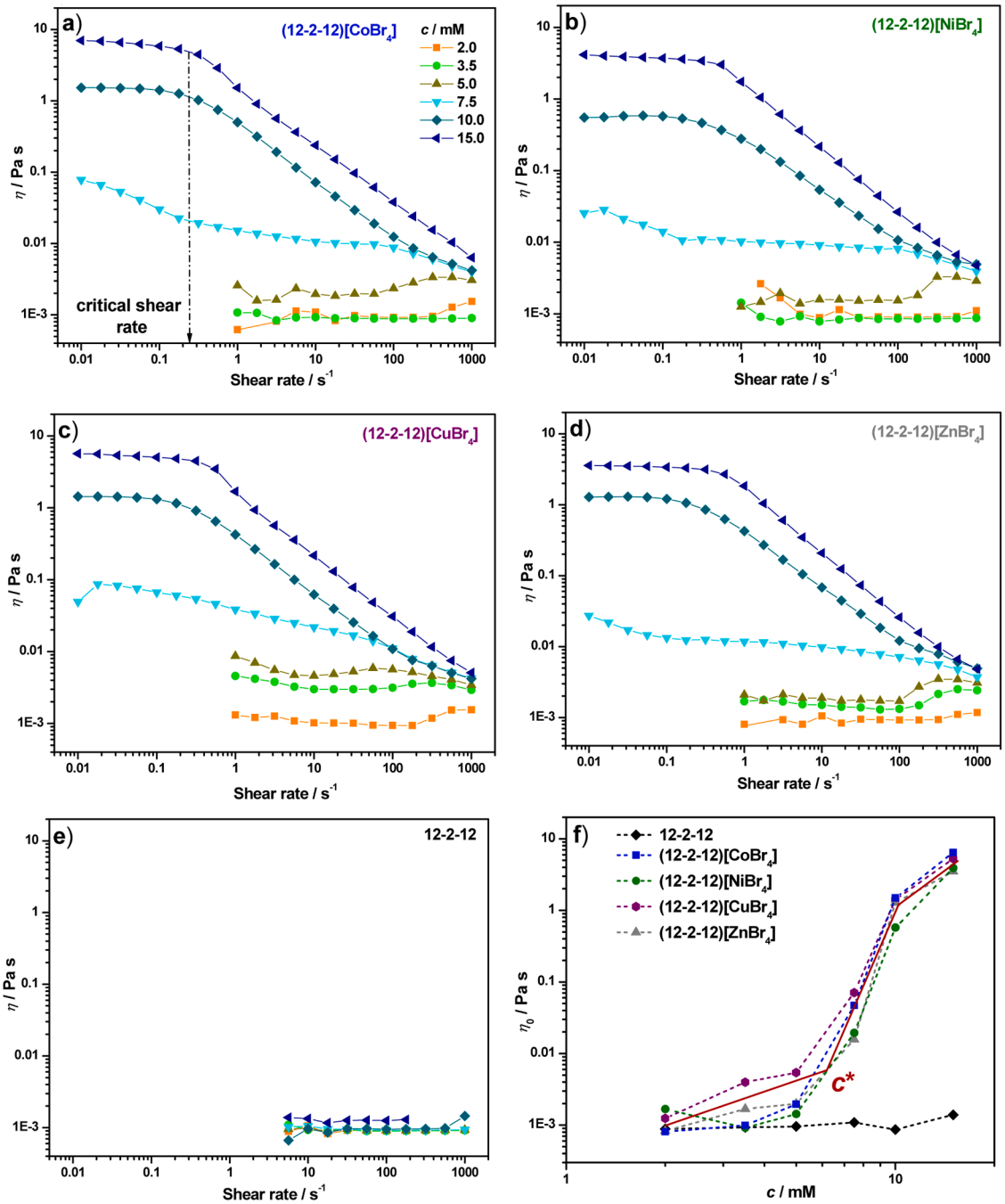


Fig. 1. a) **– e)** Shear rate ($\dot{\gamma}$) dependence of viscosity (η) over a range of concentrations (as indicated in the legend), **f)** concentration (c) dependence of zero-shear viscosity (η_0) for aqueous solutions of the dimeric metallosurfactants (12-2-12)[MBr_4], M = Co, Ni, Cu, Zn, and the metal-free precursor. All measurements were performed at 25°C. In f), the red solid line is a guide to the eye.

eradication concentration (MBEC) was determined as the lowest concentration completely preventing bacterial regrowth [30]. Time-kill assays were performed at 10, 30, and 60 minutes of exposure according to Balouiri et al. [28]. All assays were performed in duplicate on two independent occasions in aerobic conditions at 35°C.

Methodological variability of antibacterial assays is ± 1 2-fold dilution and a conservative approach was applied, whereby the final reported value corresponds to the highest value observed among all replicates. Detailed protocols are provided in the Supporting Information.

3. Results and discussion

3.1. Rheology properties

Flow behaviour and zero-shear viscosity. Shear rheology is an effective method for correlating macroscopic flow behaviour with the underlying micellar structures and their transitions, as well as for evaluating parameters relevant to further applications. Accordingly, Figs. 1. a-e) shows the variation of viscosity (η) as a function of shear rate ($\dot{\gamma}$) for different concentrations of dimeric metallosurfactants (12-2-12)[MBr_4] and corresponding precursor

12-2-12. At the lowest concentrations, all solutions exhibit very low viscosity, similar to that of water [31], and behave as Newtonian fluids, with viscosity remaining nearly constant across the applied shear rate range. For these systems, data at low shear rates are omitted because the torque signal approaches the rheometer's lower detection limit, leading to substantial noise. However, at 7.5 mM, a visible increase in viscosity is observed, and the η vs. $\dot{\gamma}$ profiles for all metallosurfactants reveal a moderate degree of shear-thinning. With further increases in concentration, i.e., at the two highest concentrations (10 and 15 mM), the viscosities increase by approximately two orders of magnitude, and the shear-thinning becomes considerably more pronounced and clearly evident in the curves. In contrast, the dimeric precursor 12-2-12 exhibits very low viscosity and behaves as a Newtonian fluid at all concentrations (Fig. 1e).

Such rheological behaviour is characteristic of WLMs, elongated and flexible surfactant aggregates that form entangled, transient networks in solution above the overlap concentration (c^*) [12,32,33]. The entanglement of WLMs imparts increased viscosity and characteristic viscoelastic properties to the solution, which are described by a model developed by Cates [34] (*vide infra*). WLM networks are dynamic, with micelles continuously breaking and reforming, hence the term "living polymers". Therefore, as the (12-2-12)[MBr_4] surfactant concentration increases, the apparent viscosity rises due to enhanced micellar entanglement, while shear thinning begins at a critical shear rate ($\dot{\gamma}_c$) as the WLMs align with the flow and the number of entanglements decreases at high shear rates [12,32].

The concentration dependence of the zero-shear viscosity (η_0) of the investigated compounds, obtained by extrapolating the viscosity curves to zero shear rate [35,36], is shown in Fig. 1f). In our previous work on the same metallosurfactant systems [21], transmission electron microscopy and dynamic light scattering revealed small, spherical or cylindrical micelles at concentrations $\leq$ 5 mM. These solutions flow readily and display low viscosity. However, once the metallosurfactant concentration exceeds 6-7 mM (Fig. 1f), η_0 increases by several orders of magnitude consistent with the formation of entangled WLMs, whereas for 12-2-12 the viscosity remains essentially unchanged over the entire concentration range. The pronounced concentration dependence observed in (12-2-12)[MBr_4] systems indicates an increase in the average length of WLMs, which is predicted by theory and consistent with literature [12,37]. All η_0 vs. c curves follow the same trend, indicating that the metal ion identity does not significantly affect the overlap concentration.

In summary, (12-2-12)[MBr_4] systems, irrespective of the metal ion, form entangled WLM networks, resulting in a significant increase in viscosity at concentrations lower than those reported for the parent surfactant, 12-2-12 [10,11,38]. For 12-2-12, Danino et al. observed viscoelastic behaviour above ~2.0 wt% (~32 mM) [11], whereas Tu et al. reported Newtonian behaviour at 30 mM in the absence of additives [38]. The shift toward lower concentrations in the metallosurfactant systems is not surprising. In solution, the $[MBr_4]^{2-}$ complex counterion dissociates into M^{2+} and Br^- ions, causing a significant increase in ionic strength relative to metal-free systems [21,39]. The heightened ionic strength more effectively screens the repulsive interactions between the quaternary ammonium headgroups, thereby promoting micellar growth and WLMs formation at lower concentrations. While it is well known that the addition of metal ions induces WLMs in surfactant solutions by screening electrostatic repulsion [40,41], the investigated systems incorporate this functionality via the tetrabromometallate counterion, offering a more cost-effective and environmentally favourable approach.

Viscoelastic Behaviour. To explore the viscoelastic properties of (12-2-12)[MBr_4] solutions, dynamic frequency sweeps were performed at the two highest concentrations (10 and 15 mM), at which the systems exhibited such behaviour. Frequency sweep tests were carried out at a constant shear strain of 10 %, selected from the linear viscoelastic range (LVER).

Figs. 2a-b) show the angular frequency (ω) dependence of the storage (elastic) modulus G' and the loss (viscous) modulus G''. At both concentrations, all curves exhibit typical viscoelastic behaviour: liquid-like ($G' < G''$) in the low-ω region and solid-like ($G' > G''$) at high-ω region. Additionally, Figs. 2c-d) present normalized Cole-Cole plots, commonly used to assess whether the viscoelastic response of WLM solutions is Maxwellian or non-Maxwellian [42]. For viscoelastic materials with single-mode Maxwell behaviour, a linear plot of G'' versus G' should be a semicircle cantered on the G' axis [36].

In both types of graphical representations, a pronounced difference is immediately noticeable between 10 and 15 mM systems, indicating a transition from non-Maxwellian to near-Maxwellian behaviour with concentration increase. Despite the polydispersity of their lengths, WLM solutions generally exhibit single-mode Maxwell behaviour, a phenomenon rationalized by Cates' late 1980s reptation-reaction theory [34,43]. Unlike polymers, WLMs are dynamic, self-assembled aggregates that continually break and recombine, providing an additional stress-relaxation pathway not present in polymer solutions. Viscoelastic relaxation of entangled WLMs occurs via two mechanisms: (a) reptation, as in polymer systems, with an associated reptation time τ_{rep}, and (b) micellar scission and recombination, characterized by a breaking time τ_{br}.

If $\tau_{br} \ll \tau_{rep}$ ("*fast-breaking limit*"), a micelle undergoes multiple scission and recombination events within the reptation timescale [34,43]. In other words, when micellar breaking/recombination is faster than reptation, the viscoelastic response becomes near-Maxwellian with a dominant relaxation time τ_R. Accordingly, the storage and loss moduli, $G'(\omega)$ and $G''(\omega)$, are well described by the single-mode Maxwell model:

$$G'(\omega) = \frac{G_0(\omega\tau_R)^2}{1+(\omega\tau_R)^2}$$

$$G''(\omega) = \frac{G_0\omega\tau_R}{1+(\omega\tau_R)^2}$$

At low ω, G' becomes proportional to ω^2 whereas G'' is proportional to ω, accordingly, the plateau modulus, G_0, and the stress relaxation time, τ_R, can therefore be deduced, respectively, from the modulus value and the crossover frequency, $G'(\omega_c) = G''(\omega_c) = G_0/2$ and $\omega_c = 1/\tau_R$.

In contrast, in the "*slow-breaking limit*" ($\tau_{br} \gtrsim \tau_{rep}$), reptation dominates and the micelles behave as polydisperse, effectively unbreakable polymers with a terminal relaxation time $\tau_{rep} \approx \tau_R$. In this regime the stress-relaxation function is non-exponential, arising from gradual

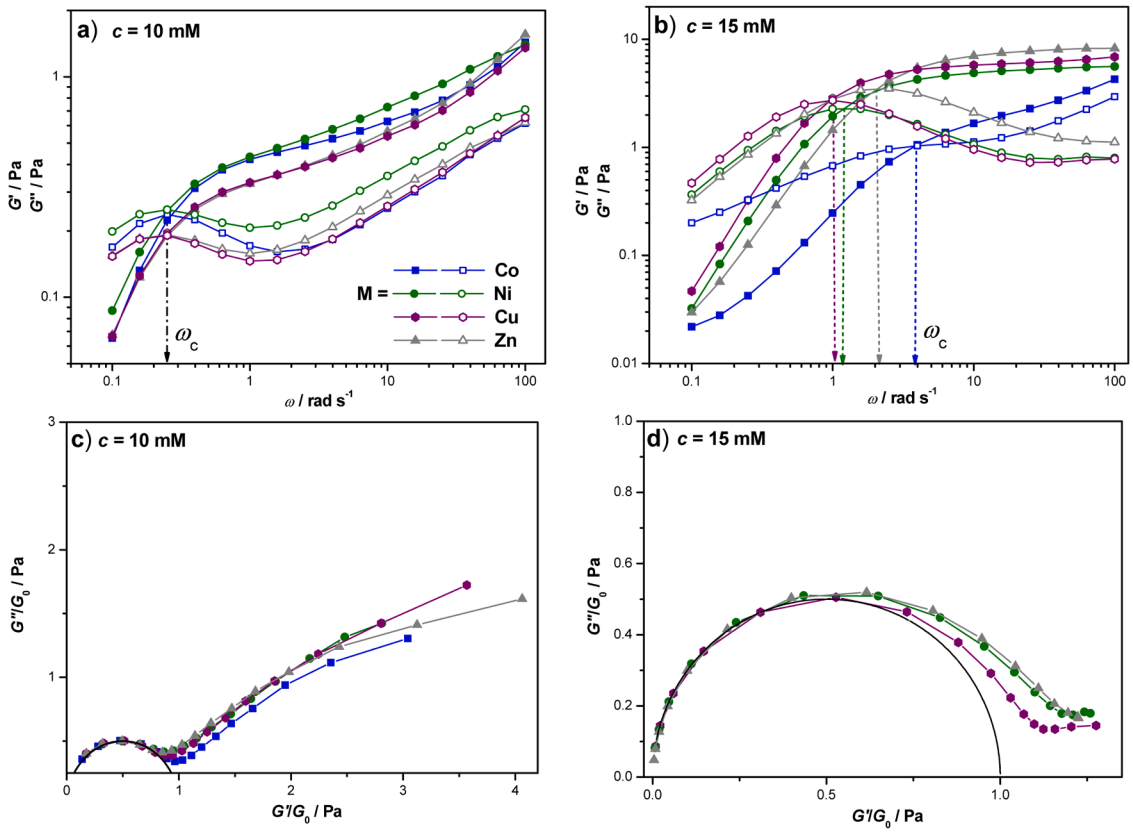


Fig. 2. a)-b) Angular frequency (ω) dependence of the storage $G'(\omega)$ (filled symbols) and loss $G''(\omega)$ (open symbols) moduli, **c)-d)** normalized Cole-Cole plots for 10 and 15 mM aqueous solutions of the dimeric metallosurfactants (12-2-12)[MBr_4], M = Co, Ni, Cu, Zn, at 25 °C. Ideal single-mode Maxwell semicircles are also shown. For the 10 mM systems (Fig. 2a), the plateau modulus G_0 used for normalization was determined from the crossover ($G' = G''$), where $G_0 = 2G'(\omega_c)$, whereas for the 15 mM systems (Fig. 2b), G_0 was obtained from single-mode Maxwell fits (see the Supporting information).

disentanglement of micellar chains within the curvilinear tube and displaying multi-mode relaxation times rather than single-mode Maxwell behaviour [33,34].

At the highest concentration, (12-2-12)[MBr_4], M = Cu, Ni, Zn, were fitted with a single-mode Maxwell model, which describes the data well (see Figs. SI-1 and Table SI-1). At high ω, all three metallosurfactants deviate from the single-mode Maxwell model due to faster relaxation processes on short time scales (Rouse or "breathing modes"), as commonly observed for WLM solutions [33,35,36]

The mesh size (ξ_m) represents the distance between entanglements in the three-dimensional WLMs network, with smaller values indicating denser entanglement and stiffer network [44,45]. For (12-2-12)[MBr_4] systems at 15 mM, the calculated ξ_m values (see Table SI-2) are comparable to or smaller than literature values for surfactant mixtures and surfactant/electrolyte systems, despite being determined at substantially lower concentrations without additives. These findings confirm that metallosurfactant systems exhibit enhanced network-forming ability, generating highly entangled WLMs at low millimolar concentrations.

In contrast to the other metallosurfactants, (12-2-12)[$CoBr_4$] shows a viscoelastic response that deviates from single-mode Maxwell behaviour at 15 mM. The Cole-Cole plot exhibits a semicircle at low ω, followed by an extended high-ω tail (see Fig. SI-2), indicating a distribution of relaxation times and/or multiple relaxation mechanisms. Shashkina *et al.* reported an analogous Cole-Cole plot for a polymer/surfactant mixture with short micelles that do not undergo scission on the reptation timescale, consistent with a multi-exponential stress-relaxation response [46]. Furthermore, at 10 mM, the Cole-Cole plots of all (12-2-12)[MBr_4] metallosurfactants (Fig. 2c) closely resemble that of (12-2-12)[$CoBr_4$]. However, the distinction between the low ω semicircle and the extended high ω arc is clearer, indicating two relaxation modes.

The distinct rheological behaviour at the two highest investigated concentrations reflects concentration-dependent micellar growth and a transition from weakly to strongly entangled WLM networks, consistent with a shift from non-Maxwellian to near-Maxwellian single-mode behaviour. The competition between scission/breakage and reptation in these systems can be expressed by the dimensionless ratio $\zeta = \tau_{br}/\tau_{rep}$ [34]. When $\tau_{br} \gtrsim \tau_{rep}$, a regime typical for short or only weakly entangled WLMs, the relaxation spectrum broadens and deviates from single-mode Maxwell behaviour. This occurs because, as the average micellar contour length L decreases, $\tau_{rep} \propto L^3$ decreases more steeply than $\tau_{br} \propto L^{-1}$ increases, driving ζ toward unity. Conversely, as micelles lengthen and entangle with increasing (12-2-12)[MBr_4] concentration, τ_{rep} increases much faster than τ_{br} decreases, and consequently $\zeta = \tau_{br}/\tau_{rep} \propto L^{-4} \ll 1$, driving the system toward fast-breaking, near-Maxwellian behaviour. Notably, at the highest concentration, (12-2-12)[$CoBr_4$] deviates from the trend observed for the other metallosurfactant systems, suggesting differences in its self-assembly behavior.

Visualization of WLMs was performed by AFM imaging (Fig. SI-3, Supporting information), which shows elongated, bundled structures characteristic of WLMs. As an example, AFM measurements were performed for (12-2-12)[$CoBr_4$]; however, no qualitative differences compared to other systems are implied, and the limitations of drying-based sample preparation must be acknowledged.

3.2. *Wettability properties*

Contact angle (θ) serves as a key metric for evaluating surfactant wetting performance, with smaller angles indicating superior wetting ability [2,47]. This property is crucial for surfactant applications, as

adequate wetting promotes uniform liquid spreading, thereby enhancing coating adhesion and cleaning efficiency due to improved surface coverage [48]. Fig. 3 shows static (sessile drop) contact angles on stainless steel at 25°C as a function of concentration for aqueous solutions of dimeric metallosurfactants and the metal-free precursor. AISI 304 stainless steel was used as the substrate, an austenitic Fe-Cr-Ni alloy (typically ~18-20 wt% Cr, ~8.0-10.5 wt% Ni) that forms a protective chromium(III) oxide passivation layer that provides oxidation and corrosion resistance [49–51]. It was chosen for wetting evaluation because of its widespread industrial, biomedical, and household applications, owing to its good corrosion resistance, mechanical strength, and processability.

The static water contact angle measured on bare stainless steel was $\theta = 59.6 \pm 2.5°$ and served as the reference. Both 12-2-12 and the metallosurfactant systems exhibit concentration-dependent behaviour in which θ decreases with increasing concentration due to surfactant adsorption and formation of an interfacial layer (Fig. 3).

For 12-2-12, θ decreases from ~ 60° to ~ 43° as concentration increases up to ~ 2 mM. Above this range (≈ 2-10 mM), θ reaches a plateau and remains nearly constant, indicating surface saturation. All metallosurfactant systems follow a similar concentration-dependent trend but generally achieve lower contact angles. At the two lowest concentrations studied, their θ values are comparable to or slightly below those of the metal-free surfactant. However, from 0.75 mM onward, the presence of the tetrabromometallate counterion leads to a more pronounced decrease in θ and thus better wettability, with minor dependence on metal ion identity. This observed trend was confirmed by statistical analysis (one-way ANOVA with Tukey's HSD post hoc test), which showed that, from 0.75 mM onward, the parent surfactant exhibits significantly higher contact angle values than all metallosurfactant systems, thus confirming the improved wettability of the metallosurfactant systems.

The concentration at which the plateau is reached exhibits only minor metal-dependent variation, ranging from 1 to 3.5 mM (Fig. 3). Accordingly, the contact angle data suggest a slightly higher cmc than the ~ 0.6 mM reported from surface tension and conductometric measurements [21], reflecting different interfacial behaviour between solid-liquid and air-liquid systems.

The observed enhanced wettability is consistent with the rheology results: dissociation of $[MBr_4]^{2-}$ increases ionic strength and screens headgroup repulsion, promoting micellar growth and WLM formation in bulk while also enabling tighter interfacial packing. In other words, the metallosurfactant systems behave as if an additional electrolyte were present, which is evidenced by the previously reported higher electrical conductivity of these metallosurfactant systems compared to the parent surfactant [21]. Furthermore, the observed colour changes upon dissolution (pale pink, green, and blue solutions) is consistent with the formation of hydrated Co^{2+}, Ni^{2+}, and Cu^{2+} species, supporting the dissociation of the complex counterions. Incorporation of the tetrabromometallate counterion thus promotes more effective wetting in the low millimolar concentration range through electrostatic shielding and tighter packing of quaternary ammonium headgroups at the stainless steel/solution interface. The formation of a more densely packed adsorbed layer is therefore consistent with the lower plateau contact angles observed for metallosurfactants compared to 12-2-12, despite similar critical micelle concentrations. A similar effect was observed in our previous work, as evidenced by the γ vs. log$c$ isotherms and the corresponding cmc values [21].

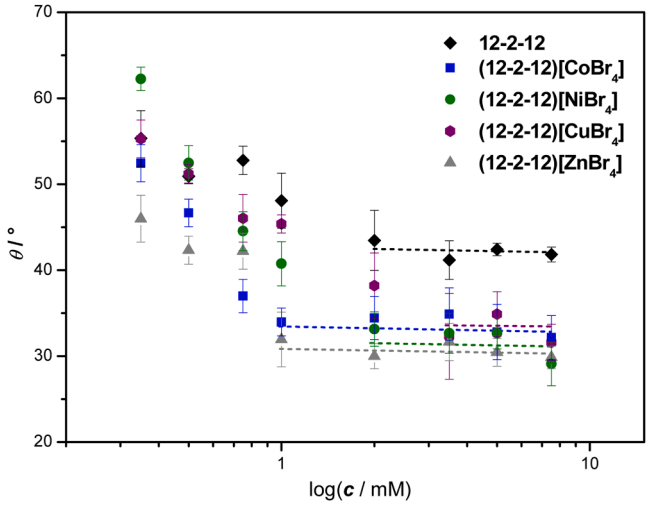


Fig. 3. Contact angle (θ) as a function of concentration (c) for aqueous solutions of the dimeric metallosurfactants (12-2-12)[MBr_4], M = Co, Ni, Cu, Zn, and the metal-free precursor on AISI 304 stainless steel at 25°C. Horizontal dashed lines indicate the plateau values for each system as a guide to the eye.

3.3. Antibacterial properties

The antibacterial activity of (12-2-12)[MBr_4] metallosurfactants was assessed by determining the antibacterial and antibiofilm efficacy parameters: MIC, MBC, BPC and MBEC (Figs. 4a-d). These metrics establish the thresholds for growth inhibition, bactericidal activity, prevention of biofilm formation, and eradication of established biofilms, respectively, enabling an in-depth characterization of the antibacterial and antibiofilm activity profile. All assays demonstrated good reproducibility with results falling within ± 1 2-fold dilution. The Figs. 4a-d) present, for each endpoint, the final results based on a conservative approach of the highest result observed. Plots showing complete data with variation between replicates are available in Supplementary information (Figs. SI4-SI8).

Biofilms exhibit intrinsic tolerance due to extracellular matrix barriers and altered cell physiology. Therefore, BPC and MBEC guide dosing and exposure conditions relevant to real-world surfaces beyond what MIC/MBC alone can predict [27,52]. All surfactants were screened against Gram-positive bacteria (*Bacillus subtilis, Staphylococcus aureus*) and Gram-negative bacteria (*Escherichia coli, Pseudomonas aeruginosa*). Both the metal-free precursor and metallosurfactants demonstrated potent antibacterial efficacy against planktonic and biofilm populations, i.e., all compounds achieved very low effective concentrations in the micromolar range (Figs. 4a-d).

Across all tested organisms, metallosurfactants exhibited bactericidal activity according to the standard MBC/MIC criterion (MBC/MIC ≤ 4) [53,54]. In most cases, MBC equaled MIC (MBC/MIC = 1) and at most was twofold higher (MBC/MIC = 2). The compounds showed the highest efficacy against *B. subtilis* and *S. aureus*, intermediate activity against *E. coli*, and the lowest effectiveness against *P. aeruginosa*. This susceptibility ranking aligns with established biocide literature [55,56]. Gram-positive bacteria generally show greater susceptibility to cationic biocides than Gram-negative species due to the absence of an outer membrane. *E. coli* exhibits intermediate susceptibility, while *P. aeruginosa* exhibits greater tolerance due to low outer membrane permeability and active efflux mechanisms [55–57].

No significant differences in MIC or MBC were observed among the tested surfactants, irrespective of the incorporated metal. Moreover, the differences between the metal-free precursor and the metallosurfactants were negligible (i.e., within a twofold dilution), indicating that the amphiphilic $(12\text{-}2\text{-}12)^{2+}$ cation drives antibacterial activity.

The MICs determined for the parent dimeric surfactant, 12-2-12, were markedly lower than those previously reported [58–60], which also differ among studies. This likely reflects methodological differences such as assay format (broth microdilution vs. agar dilution), growth medium, inoculum density, and stock solvent, underscoring the need for standardized testing protocols [61,62]. Existing literature on related metallosurfactants predominantly reports zones of inhibition rather than broth microdilution assays for MIC and MBC determinations

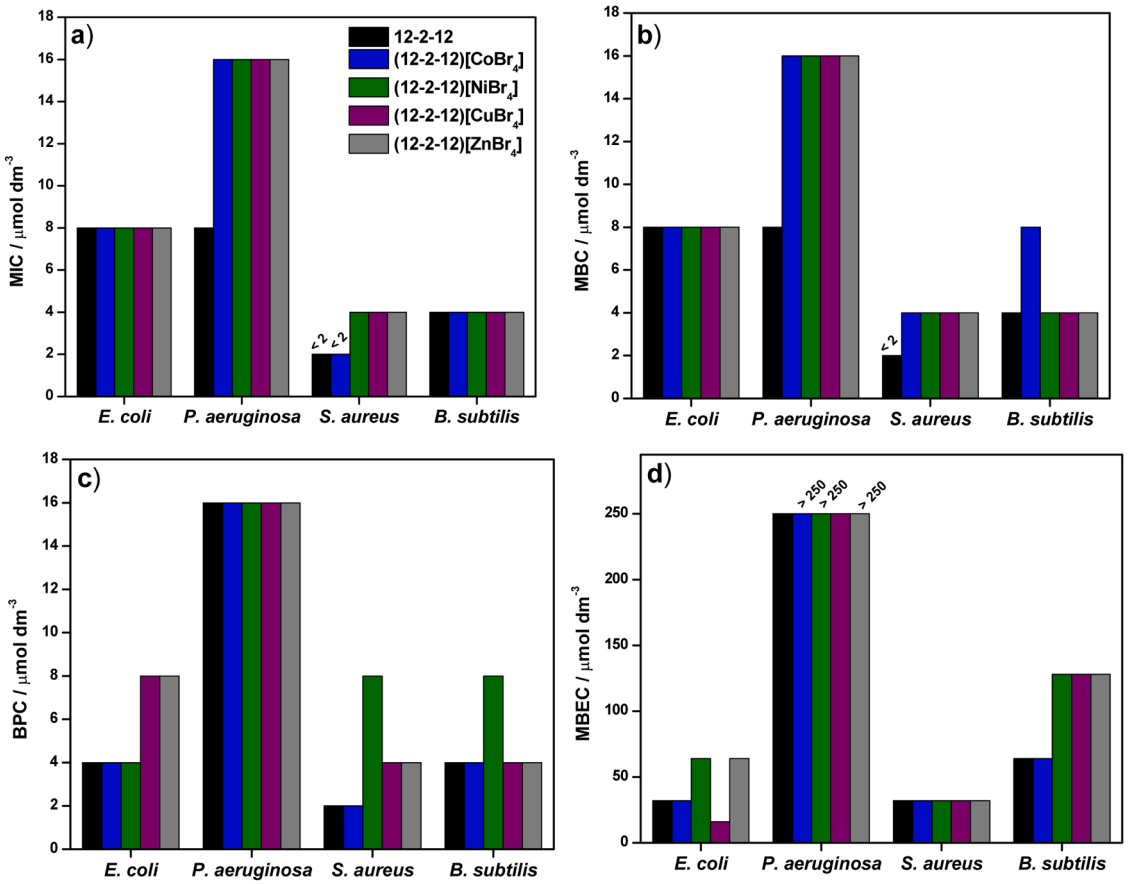


Fig. 4. Antibacterial and antibiofilm parameters: minimum inhibitory concentration (MIC), minimum bactericidal concentration (MBC), biofilm prevention concentration (BPC) and minimum biofilm eradication concentration (MBEC) for (12-2-12)[MBr_4] M = Co, Ni, Cu, Zn, metallosurfactants and the metal-free precursor against four bacterial strains: *Bacillus subtilis, Staphylococcus aureus, Escherichia coli* and *Pseudomonas aeruginosa*.

[16–18].

Antibiofilm activity assays revealed that MBEC values consistently exceeded BPC values across all tested organisms and metallosurfactants, reflecting the much greater difficulty of eradicating established biofilms compared to preventing their formation (Fig. 4c-d), consistent with previously reported findings [27,52]. *P. aeruginosa* demonstrated the highest resistance, with uniform BPC values of 16 μM and MBEC values exceeding the assay upper limit of 250 μM for all compounds except for the parent surfactant, 12-2-12, and (12-2-12)[$CuBr_4$]. For *S. aureus, E. coli*, and *B. subtilis*, BPC values remained consistent across all surfactants within two twofold dilution steps (2-8 μM). Such species-dependent differences in antibacterial effects have been long known for various biocides [55,56]. A similar trend was observed for MBEC, with minimal differences between surfactants across these three species.

Time-kill assays with a concentration-time approach provide practical advantages by combining optimal dosing regimens with the exposure time needed for applications such as surface disinfection. As expected, the required concentrations generally decreased with longer exposure, although the observed trend varied across bacterial species and metallosurfactants (Figs. 5a-d). *P. aeruginosa* demonstrated the highest resistance at all time points, requiring the assay upper limit of 250 μM or higher at 10 and 30 minutes for all compounds. At 60 minutes, (12-2-12)[MBr_4] (M = Zn, Cu, Ni) achieved killing at 32 μM, whereas the metal-free precursor and (12-2-12)[$CoBr_4$] remained at 250 μM, indicating superior time-dependent efficacy for the former. *E. coli* showed moderate initial resistance (64-125 μM) at 10 min, with (12-2-12)[$ZnBr_4$] requiring the highest concentration for bactericidal activity, but all compounds converged to 16 μM at 30 minutes. Following a 1 h exposure, the lethal concentrations further decreased to 4-8 μM, substantially lower than those required for *P. aeruginosa*. Both Gram-positive species exhibited rapid bactericidal kinetics. Low lethal concentrations (2-8 μM) were sufficient at all time points and remained consistent across all tested surfactants within two twofold dilution steps. The only exceptions were (12-2-12)[$NiBr_4$] against *B. subtilis* and (12-2-12)[$CuBr_4$] against *S. aureus* at 10 min, which exhibited slightly reduced bactericidal efficacy. These findings mirror the MIC/MBC trends observed herein: highest potency for Gram-positive bacteria (*B. subtilis, S. aureus*), moderate for *E. coli*, and lowest for *P. aeruginosa*. Similarly, the time-kill assay confirms that the nature of the incorporated metal does not significantly affect antibacterial activity.

It is well known that quaternary ammonium surfactants are broad-spectrum antibacterial agents whose mechanism of action involves electrostatic binding to the bacterial cell membrane and penetration by hydrocarbon chains, leading to cumulative hydrophobic and electrostatic adsorption at the membrane/water interface [4,8,56,63]. Subsequent destabilization and permeabilization of the membrane ultimately result in lysis and cell death. Dimeric surfactants follow the same fundamental mechanism and achieve equivalent or superior killing at lower molar concentrations compared to monomeric analogues due to their dicationic nature and two-tailed structure, resulting in stronger interactions with bacterial membranes [7,8]. On the other hand, metal ions can exist as multiple chemical species and inhibit bacterial growth through oxidative stress, protein dysfunction, and membrane damage [64]. Moreover, uptake routes and intracellular targeting are shaped by metal speciation, with non-essential metals often entering via transporters that normally acquire essential inorganic and organic ions. Given the rapid worldwide emergence of resistant microbes, compounds that combine multiple antibacterial mechanisms with enhanced

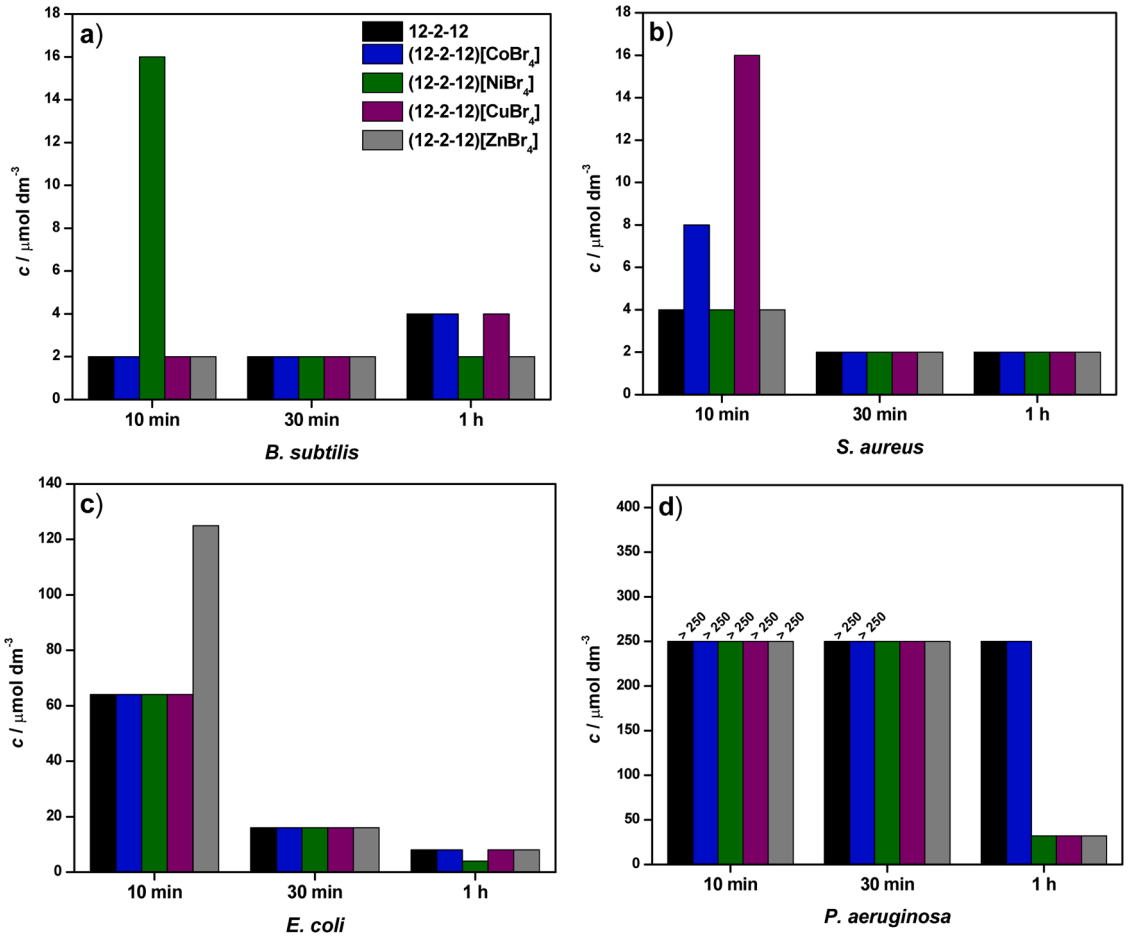


Fig. 5. Time dependent antibacterial activity of (12-2-12)[MBr_4], M = Co, Ni, Cu, Zn metallosurfactants and the metal-free precursor: minimum concentrations required for complete inhibition of bacterial growth against four bacterial strains at exposure times of 10 min, 30 min, and 1 h.

antibacterial efficacy, such as dimeric metallosurfactants (12-2-12)[MBr_4], are of particular interest owing to their reduced tendency to promote antimicrobial resistance.

4. Conclusions

This work establishes counterion engineering as a versatile strategy for modulating surfactant performance across multiple functional domains. The substitution of bromide with the tetrabromometallate counterion in the dimeric 12-2-12 surfactant increases the ionic strength of the systems and promotes micellar transitions from spherical to cylindrical to wormlike structures. The increased ionic strength screens electrostatic repulsions between headgroups, thereby promoting micellar growth and entanglement. This shifts the onset of viscoelasticity to the low millimolar range, independent of the metal centre and without the need for additives or co-surfactants. A concentration increase from 10 to 15 mM leads to a transition from non-Maxwellian to near-Maxwellian behaviour, reflecting the formation of more strongly entangled WLM networks. The same mechanism enables tighter molecular packing at the stainless-steel/solution interface and thereby promotes more effective wetting at low millimolar concentrations.

All complexes exhibit pronounced antibacterial and antibiofilm performance at low micromolar concentrations. The four metallosurfactants and the metal-free precursor show comparable MIC and MBC values, indicating that antibacterial activity is primarily governed by the quaternary ammonium cations $(12\text{-}2\text{-}12)^{2+}$ rather than the identity of the metal centre. Time-kill and antibiofilm assays further demonstrate broad-spectrum efficacy, while highlighting the increased tolerance of mature biofilms.

Overall, the structure-property relationships established here show that tetrabromometallate counterions modulate micellar structure and interfacial behaviour through ionic strength effects, while antibacterial and antibiofilm activities primarily originate from the amphiphilic dication $(12\text{-}2\text{-}12)^{2+}$ and its membrane-disruptive mechanism. From an application-oriented perspective, these metallosurfactants offer a combination of properties relevant to antimicrobial coating development: (i) viscoelastic behaviour at low concentrations, which can reduce material consumption, (ii) enhanced wetting on metallic substrates, supporting improved processability, (iii) broad-spectrum antibacterial and antibiofilm efficacy at micromolar concentrations, providing effective antimicrobial functionality. The straightforward synthesis (high yields, ambient conditions) and chemical stability further support their potential for practical implementation.

While the tetrabromometallate counterion governs the investigated rheological and wetting properties, the metal centre itself has only a modest effect. This design flexibility enables metal selection based on desired additional functionalities: catalytic, magnetic, or optical, without compromising the established surfactant performance. Taken together, these attributes highlight dimeric metallosurfactants as adaptable platforms for antimicrobial coating formulations and other functional surface active systems.

Funding

This work was fully financially supported by the Croatian Science Foundation under project number IP-2024-05-3668, *MSurf-n-SWIM*, and

by the European Union's Horizon Europe RIA project *Surface Transfer of Pathogens (STOP)*, Grant Agreement ID: 101057961. We also acknowledge the support of the project co-financed by the Croatian Government and the European Union through the European Regional Development Fund - the Competitiveness and Cohesion Operational Programme: Sustainable bioprospecting of organisms from the Adriatic Sea for innovative natural products (PK 1.1.10.0001) within the Center of Research Excellence for Marine Bioprospecting – BioProCro (PK 1.1.10).

During the preparation of this work the author(s) used ChatGPT in order to assist with grammar and spelling correction of the manuscript text. After using this tool/service, the author(s) reviewed and edited the content as needed and take(s) full responsibility for the content of the published article.

CRediT authorship contribution statement

Ana Ivančić: Writing – original draft, Visualization, Project administration, Investigation, Data curation. **Krunoslav Bojanić:** Validation, Methodology, Investigation, Formal analysis, Data curation. **Mirna Perkušić:** Validation, Methodology, Investigation, Formal analysis, Data curation. **Ivana Tartaro Bujak:** Methodology, Investigation. **Katarina Marušić:** Methodology, Investigation. **Nives Novosel Vlašić:** Investigation. **Tea Mišić Radić:** Methodology. **Darija Domazet Jurašin:** Writing – review & editing, Writing – original draft, Visualization, Investigation, Funding acquisition, Conceptualization.

Declaration of competing interest

The authors declare that they have no known competing financial interests or personal relationships that could have appeared to influence the work reported in this paper.

Supplementary materials

Supplementary material associated with this article can be found, in the online version, at doi:10.1016/j.ceja.2026.101190.

Data availability

Data will be made available on request.

References

[1] C. Fong, T. Le, C.J. Drummond, Lyotropic liquid crystal engineering–ordered nanostructured small molecule amphiphileself-assembly materials by design, Chem. Soc. Rev. 41 (2012) 1297–1322, https://doi.org/10.1039/C1CS15148G.
[2] I.Batool Aisha, S. Iftekhar, M.B. Taj, S.A.C. Carabineiro, F. Ahmad, M.I. Khan, A. Shanableh, H. Alshater, Wetting the surface: a deep dive into chemistry and applications of surfactants, Clean. Chem. Eng. 11 (2025) 100197, https://doi.org/10.1016/j.clce.2025.100197.
[3] P. Shenoy, N. Kedimar, S.A. Rao, A comprehensive review on anticorrosive behaviour of surfactants across diverse metals using multiple techniques: current insights and future horizons, Chem. Eng. J. Adv. 20 (2024) 100645, https://doi.org/10.1016/j.ceja.2024.100645.
[4] M.C. Jennings, K.P.C. Minbiole, W.M. Wuest, Quaternary Ammonium Compounds: An Antimicrobial Mainstay and Platform for Innovation to Address Bacterial Resistance, ACS Infect. Dis. 1 (2015) 288–303, https://doi.org/10.1021/acsinfecdis.5b00047.
[5] A. Gbadamosi, S.O. Badmus, K. Haruna, S. Patil, M.S. Kamal, M. Mahmoud, T. A. Saleh, Surfactant applications in oil and gas industry: Efficiency, toxicity, and remediation techniques, J. Mol. Liq. 427 (2025) 127440, https://doi.org/10.1016/j.molliq.2025.127440.
[6] R. Sharma, A. Kamal, M. Abdinejad, R.K. Mahajan, H.-B. Kraatz, Advances in the synthesis, molecular architectures and potential applications of gemini surfactants, Adv. Colloid Interface Sci. 248 (2017) 35–68, https://doi.org/10.1016/j.cis.2017.07.032.
[7] A.R. Ahmady, P. Hosseinzadeh, A. Solouk, S. Akbari, A.M. Szulc, B.E. Brycki, Cationic gemini surfactant properties, its potential as a promising bioapplication candidate, and strategies for improving its biocompatibility: A review, Adv. Colloid Interface Sci. 299 (2022) 102581, https://doi.org/10.1016/j.cis.2021.102581.
[8] B.E. Brycki, I.H. Kowalczyk, A.M. Szulc, J.A. Brycka, Quaternary Alkylammonium Salts as Cleaning and Disinfectant Agents, Tenside Surfactants Deterg. 55 (2018) 432–438, https://doi.org/10.3139/113.110592.
[9] R. Zana, Dimeric and oligomeric surfactants. Behavior at interfaces and in aqueous solution: a review, Adv. Colloid Interface Sci. 97 (2002) 205–253, https://doi.org/10.1016/S0001-8686(01)00069-0.
[10] A. Bernheim-Groswasser, R. Zana, Y. Talmon, Sphere-to-Cylinder Transition in Aqueous Micellar Solution of a Dimeric (Gemini) Surfactant, J. Phys. Chem. B 104 (2000) 4005–4009, https://doi.org/10.1021/jp994301a.
[11] D. Danino, Y. Talmon, R. Zana, Alkanediyl-alfa, omega-bis (dimethylalkyammonium bromide) Surfactants (Dimeric Surfactants). 5. Aggregation and Microstructure in Aqueous Solutions, Langmuir 11 (1995) 1448–1456, https://doi.org/10.1021/la00005a008.
[12] K. Morishima, S. Sugawara, T. Yoshimura, M. Shibayama, Structure and Rheology of Wormlike Micelles Formed by Fluorocarbon–Hydrocarbon-Type Hybrid Gemini Surfactant in Aqueous Solution, Langmuir 33 (2017) 6084–6091, https://doi.org/10.1021/acs.langmuir.7b00902.
[13] J.P. Rothstein, H. Mohammadigoushki, Complex flows of viscoelastic wormlike micelle solutions, J. Non-Newton. Fluid Mech. 285 (2020) 104382, https://doi.org/10.1016/j.jnnfm.2020.104382.
[14] J. Yang, Viscoelastic wormlike micelles and their applications, Curr. Opin. Colloid Interface Sci. 7 (2002) 276–281, https://doi.org/10.1016/S1359-0294(02)00071-7.
[15] S. Kumari, M. Nehra, S. Jain, N. Dilbaghi, G.R. Chaudhary, K.-H. Kim, S. Kumar, Metallosurfactant aggregates: Structures, properties, and potentials for multifarious applications, Adv. Colloid Interface Sci. 323 (2024) 103065, https://doi.org/10.1016/j.cis.2023.103065.
[16] G. Kaur, S. Kumar, N. Dilbaghi, G. Bhanjana, S.K. Guru, S. Bhushan, S. Jaglan, P. A. Hassan, V.K. Aswal, Hybrid surfactants decorated with copper ions: aggregation behavior, antimicrobial activity and anti-proliferative effect, Phys. Chem. Chem. Phys 18 (2016) 23961–23970, https://doi.org/10.1039/C6CP03070J.
[17] G. Kaur, P. Garg, B. Kaur, G.R. Chaudhary, S. Kumar, N. Dilbaghi, P.A. Hassan, S. L. Gawali, Cationic double chained metallosurfactants: synthesis, aggregation, cytotoxicity, antimicrobial activity and their impact on the structure of bovine serum albumin, Soft Matter 14 (2018) 5306–5318, https://doi.org/10.1039/C8SM00535D.
[18] S. Veeralakshmi, S. Nehru, S. Arunachalam, P. Kumar, M. Govindaraju, Study of single and double chain surfactant–cobalt(III) complexes and their hydrophobicity, micelle formation, interaction with serum albumins and antibacterial activities, Inorg. Chem. Front 1 (2014) 393–404, https://doi.org/10.1039/C4QI00018H.
[19] H. Mehta, G. Kaur, G.Ram Chaudhary, Environmentally benign fouling release metallosurfactant coatings; evaluation of surface properties, leaching rate, biocorrosion resistance and durability, Appl. Surf. Sci. 635 (2023) 157726, https://doi.org/10.1016/j.apsusc.2023.157726.
[20] H. Mehta, G. Kaur, G.R. Chaudhary, N. Prabhakar, S. Kaul, N.K. Singhal, Evaluation of corrosion resistant, antimicrobial and cytocompatible behaviour of cobalt based metallosurfactants self-assembled monolayers on 316L stainless steel surface, Surf. Coat. Technol. 444 (2022) 128657, https://doi.org/10.1016/j.surfcoat.2022.128657.
[21] M. Rubčić, M. Herak, L. Zagorec, D.Domazet Jurašin, Transition Metal-Based Dimeric Metallosurfactants: From Organic–Inorganic Hybrid Structures and Low-Dimensional Magnets to Metallomicelles, Inorg. Chem 63 (2024) 12218–12230, https://doi.org/10.1021/acs.inorgchem.4c01550.
[22] J.A. Kitchen, N.G. White, G.N.L. Jameson, J.L. Tallon, S. Brooker, Effect of Counteranion X on the Spin Crossover Properties of a Family of Diiron(II) Triazole Complexes $[Fe^{II}_2(PMAT)_2](X)_4$, Inorg. Chem 50 (2011) 4586–4597, https://doi.org/10.1021/ic200308k.
[23] M.A. Butt, Thin-Film Coating Methods: A Successful Marriage of High-Quality and Cost-Effectiveness—A Brief Exploration, Coatings 12 (2022) 1115, https://doi.org/10.3390/coatings12081115.
[24] P.C. Uzoma, I.-I.N. Etim, B.O. Okonkwo, O.S. Olanrele, D.I. Njoku, S.K. Kolawole, W. Emori, A.I. Ikeuba, C.N. Njoku, O.O. Ekerenam, I.P. Etim, E.F. Daniel, I.I. Udoh, Recent design approaches, adhesion mechanisms, and applications of antibacterial surfaces, Chem. Eng. J. Adv. 16 (2023) 100563, https://doi.org/10.1016/j.ceja.2023.100563.
[25] D. Jurašin, I. Habuš, N. Filipović-Vinceković, Role of the alkyl chain number and head groups location on surfactants self-assembly in aqueous solutions, Colloids Surf. A: Physicochem. Eng. Asp. 368 (2010) 119–128, https://doi.org/10.1016/j.colsurfa.2010.07.025.
[26] European Committee for Antimicrobial Susceptibility Testing (EUCAST) of the European Society of Clinical Microbiology and Infectious Diseases (ESCMID), Determination of minimum inhibitory concentrations (MICs) of antibacterial agents by broth dilution, Clin. Microbiol. Infect. 9 (2003) 1–7, https://doi.org/10.1046/j.1469-0691.2003.00790.x.
[27] M.D. Macia, E. Rojo-Molinero, A. Oliver, Antimicrobial susceptibility testing in biofilm-growing bacteria, Clin. Microbiol. Infect. 20 (2014) 981–990, https://doi.org/10.1111/1469-0691.12651.
[28] M. Balouiri, M. Sadiki, S.K. Ibnsouda, Methods for in vitro evaluating antimicrobial activity: A review, J. Pharm. Anal. 6 (2016) 71–79, https://doi.org/10.1016/j.jpha.2015.11.005.
[29] S. Stepanović, D. Vuković, V. Hola, G.D. Bonaventura, S. Djukić, I. Ćirković, F. Ruzicka, Quantification of biofilm in microtiter plates: overview of testing conditions and practical recommendations for assessment of biofilm production by staphylococci, APMIS 115 (2007) 891–899, https://doi.org/10.1111/j.1600-0463.2007.apm_630.x.
[30] L. Thieme, A. Hartung, K. Tramm, M. Klinger-Strobel, K.D. Jandt, O. Makarewicz, M.W. Pletz, MBEC Versus MBIC: the Lack of Differentiation between Biofilm Reducing and Inhibitory Effects as a Current Problem in Biofilm Methodology, Biol Proced Online 21 (2019) 18, https://doi.org/10.1186/s12575-019-0106-0.

[31] M.L. Huber, R.A. Perkins, A. Laesecke, D.G. Friend, J.V. Sengers, M.J. Assael, I. N. Metaxa, E. Vogel, R. Mareš, K. Miyagawa, New International Formulation for the Viscosity of H2O, J. Phys. Chem. Ref. Data 38 (2009) 101–125, https://doi.org/10.1063/1.3088050.
[32] C.A. Dreiss, Chapter 1. Wormlike Micelles: An Introduction, in: C.A. Dreiss, Y. Feng (Eds.), Soft Matter Series, Royal Society of Chemistry, Cambridge, 2017, pp. 1–8, https://doi.org/10.1039/9781782629788-00001.
[33] C.A. Dreiss, Wormlike micelles: where do we stand? Recent developments, linear rheology and scattering techniques, Soft Matter 3 (2007) 956, https://doi.org/10.1039/b705775j.
[34] M.E. Cates, S.M. Fielding, Rheology of giant micelles, Adv. Phys. 55 (2006) 799–879, https://doi.org/10.1080/00018730601082029.
[35] K. Aramaki, S. Hoshida, S. Arima, Formation of wormlike micelles with natural-sourced ingredients (sucrose fatty acid ester and fatty acid) and a viscosity-boosting effect induced by fatty acid soap, Colloids Surf. A: Physicochem. Eng. Asp. 396 (2012) 278–282, https://doi.org/10.1016/j.colsurfa.2012.01.009.
[36] D.P. Acharya, H. Kunieda, Wormlike micelles in mixed surfactant solutions, Adv. Colloid Interface Sci. 123–126 (2006) 401–413, https://doi.org/10.1016/j.cis.2006.05.024.
[37] R. Oda, P. Panizza, M. Schmutz, F. Lequeux, Direct Evidence of the Shear-Induced Structure of Wormlike Micelles: Gemini Surfactant 12−2−12, Langmuir 13 (1997) 6407–6412, https://doi.org/10.1021/la9621170.
[38] Y. Tu, M. Gao, H. Teng, Y. Shang, B. Fang, H. Liu, A gemini surfactant-containing system with abundant self-assembly morphology and rheological behaviors tunable by photoinduction, RSC Adv 8 (2018) 16004–16012, https://doi.org/10.1039/C8RA01070F.
[39] R. Kaur, S. Gupta, S.K. Mehta, Y. Imai, T. Takiue, H. Matsubara, M. Aratono, Probing the self-aggregation behavior and counter ion distribution of a copper surfactant complex, New J. Chem 38 (2014) 3925–3932, https://doi.org/10.1039/C4NJ00620H.
[40] E. Warmbier-Wytykowska, A.P. Williams, J. Rozanski, P. Fischer, V. Lutz-Bueno, S. Handschin, L. Baraldi, J. Warmbier, P. Wagner, S. Różańska, How Do the Valency and Radii of Cations Affect the Rheological Properties of Aqueous Solutions of Zwitterionic and Anionic Surfactant Mixtures? Langmuir 41 (2025) 3561–3571, https://doi.org/10.1021/acs.langmuir.4c04689.
[41] Z. Mitrinova, Z. Valkova, S. Tcholakova, Interplay between cosurfactants and electrolytes for worm-like micelles formation, Colloids Surf. A: Physicochem. Eng. Asp. 707 (2025) 135943, https://doi.org/10.1016/j.colsurfa.2024.135943.
[42] N.R. Agrawal, X. Yue, S.R. Raghavan, The Unusual Rheology of Wormlike Micelles in Glycerol: Comparable Timescales for Chain Reptation and Segmental Relaxation, Langmuir 36 (2020) 6370–6377, https://doi.org/10.1021/acs.langmuir.0c00489.
[43] M.E. Cates, Reptation of living polymers: dynamics of entangled polymers in the presence of reversible chain-scission reactions, Macromolecules 20 (1987) 2289–2296, https://doi.org/10.1021/ma00175a038.
[44] B.A. Schubert, E.W. Kaler, N.J. Wagner, The Microstructure and Rheology of Mixed Cationic/Anionic Wormlike Micelles, Langmuir 19 (2003) 4079–4089, https://doi.org/10.1021/la020821c.
[45] Y. Zhao, S.J. Haward, A.Q. Shen, Rheological characterizations of wormlike micellar solutions containing cationic surfactant and anionic hydrotropic salt, J. Rheol. 59 (2015) 1229–1259, https://doi.org/10.1122/1.4928454.
[46] J.A. Shashkina, O.E. Philippova, Y.D. Zaroslov, A.R. Khokhlov, T.A. Pryakhina, I. V. Blagodatskikh, Rheology of Viscoelastic Solutions of Cationic Surfactant. Effect of Added Associating Polymer, Langmuir 21 (2005) 1524–1530, https://doi.org/10.1021/la0482756.
[47] T. Huhtamäki, X. Tian, J.T. Korhonen, R.H.A. Ras, Surface-wetting characterization using contact-angle measurements, Nat. Protoc. 13 (2018) 1521–1538, https://doi.org/10.1038/s41596-018-0003-z.
[48] N.M. Kovalchuk, M.J.H. Simmons, Surfactant-mediated wetting and spreading: Recent advances and applications, Curr. Opin. Colloid Interface Sci. 51 (2021) 101375, https://doi.org/10.1016/j.cocis.2020.07.004.
[49] C. Örnek, B. Payam, A. Gloskovskii, K. Kazmanlı, N. Mohamed, B. Derin, M. Ürgen, C.-E. Chou, H.-W. Yen, B. Avcı, S. Ooi, Understanding the passive behaviour of low-chromium high-strength Hybrid steel in corrosive environments, Npj Mater Degrad 7 (2023) 71, https://doi.org/10.1038/s41529-023-00392-z.
[50] P. Taxell, P. Huuskonen, Toxicity assessment and health hazard classification of stainless steels, Regul. Toxicol. Pharmacol. 133 (2022) 105227, https://doi.org/10.1016/j.yrtph.2022.105227.
[51] X. Zhao, Z. Li, B. Yang, X. Sun, G. Sun, S. Wang, C. Chen, Microstructure and mechanical properties of 304 stainless steel produced by interpass milling hybrid direct energy deposition-arc, J. Mater. Res. Technol. 27 (2023) 3744–3756, https://doi.org/10.1016/j.jmrt.2023.10.137.
[52] T. Coenye, Biofilm antimicrobial susceptibility testing: where are we and where could we be going? Clin. Microbiol. Rev. 36 (2023) e00024 https://doi.org/10.1128/cmr.00024-23, 23.
[53] N. Wald-Dickler, P. Holtom, B. Spellberg, Busting the Myth of "Static vs Cidal": A Systemic Literature Review, Clin. Infect. Dis. 66 (2018) 1470–1474, https://doi.org/10.1093/cid/cix1127.
[54] K. Bielawski, K. Leszczyńska, Z. Kałuża, A. Bielawska, O. Michalak, T. Daniluk, O. Staszewska-Krajewska, A. Czajkowska, N. Pawłowska, A. Gornowicz, Synthesis and antimicrobial activity of chiral quaternary N-spiro ammonium bromides with 3′,4′-dihydro-1′h-spiro[isoindoline-2,2′isoquinoline] skeleton, DDDT 11 (2017) 2015–2028, https://doi.org/10.2147/DDDT.S133250.
[55] J.M. Boyce, Quaternary ammonium disinfectants and antiseptics: tolerance, resistance and potential impact on antibiotic resistance, Antimicrob. Resist. Infect. Control. 12 (2023) 32, https://doi.org/10.1186/s13756-023-01241-z.
[56] G. McDonnell, A.D. Russell, Antiseptics and disinfectants: activity, action, and resistance, Clin. Microbiol. Rev. 12 (1999) 147–179, https://doi.org/10.1128/CMR.12.1.147.
[57] Y. Morita, J. Tomida, Y. Kawamura, Responses of Pseudomonas aeruginosa to antimicrobials, Front. Microbiol. 4 (2014), https://doi.org/10.3389/fmicb.2013.00422.
[58] K. Kuperkar, J. Modi, K. Patel, Surface-active properties and antimicrobial study of conventional cationic and synthesized symmetrical gemini surfactants, J Surfact Deterg. 15 (2012) 107–115, https://doi.org/10.1007/s11743-011-1269-0.
[59] S. Zhang, S. Ding, J. Yu, X. Chen, Q. Lei, W. Fang, Antibacterial activity, *in vitro* cytotoxicity, and cell cycle arrest of gemini quaternary ammonium surfactants, Langmuir 31 (2015) 12161–12169, https://doi.org/10.1021/acs.langmuir.5b01430.
[60] A. Laatiris, M. El Achouri, M. Rosa Infante, Y. Bensouda, Antibacterial activity, structure and CMC relationships of alkanediyl α,ω-bis(dimethylammonium bromide) surfactants, Microbiol. Res. 163 (2008) 645–650, https://doi.org/10.1016/j.micres.2006.09.006.
[61] M. Bubonja-Šonje, S. Knežević, M. Abram, Challenges to antimicrobial susceptibility testing of plant-derived polyphenolic compounds, Arch. Ind. Hyg. Toxicol. 71 (2020) 300–311, https://doi.org/10.2478/aiht-2020-71-3396.
[62] S. Štumpf, G. Hostnik, M. Primožič, M. Leitgeb, J.-P. Salminen, U. Bren, The effect of growth medium strength on minimum inhibitory concentrations of tannins and tannin extracts against E. coli, Molecules 25 (2020) 2947, https://doi.org/10.3390/molecules25122947.
[63] N. Hanheiser, Y. Jiang, C. Nie, R. Haag, Mechanism and molecular design principles of cationic surfactants: from charge-driven membrane interactions to next-generation quaternary ammonium compounds, ChemMedChem 21 (2026) e202501104, https://doi.org/10.1002/cmdc.202501104.
[64] J.A. Lemire, J.J. Harrison, R.J. Turner, Antimicrobial activity of metals: mechanisms, molecular targets and applications, Nat. Rev. Microbiol. 11 (2013) 371–384, https://doi.org/10.1038/nrmicro3028.